Published in final edited form as:
Mol Ther. 2006 July ; 14(1): 69–78. doi:10.1016/j.ymthe.2006.02.018.

The "Perivascular Pump" Driven by Arterial Pulsation is a Powerful Mechanism for the Distribution of Therapeutic Molecules within the Brain

Piotr Hadaczek[1,*], **Yoji Yamashita**[1], **Hanna Mirek**[1], **Laszlo Tamas**[2], **Martha C. Bohn**[3], **Charles Noble**[4], **John W. Park**[4], and **Krystof Bankiewicz**[1]

[1]Laboratory of Molecular Therapeutics, Department of Neurological Surgery, UCSF, MCB, 1855 Folsom Street, Room 226, San Francisco, CA 94103, USA

[2]Pacific Neurosciences Institute, Orinda, CA 94563, USA

[3]Neurobiology Program, Department of Pediatrics, Children's Memorial Research Center, Feinberg School of Medicine, Northwestern University, Chicago, IL 60614, USA

[4]University of California at San Francisco Comprehensive Cancer Center, San Francisco, CA 94115, USA

Abstract

We investigated the movement of interstitially infused macromolecules within the central nervous system (CNS) in rats with high and low blood pressure (BP)/heart rate and in rats euthanized immediately before infusion (no heart action). Adeno-associated virus 2 (AAV2), fluorescent liposomes, or bovine serum albumin was infused into rat striatum (six hemispheres per group) by convection-enhanced delivery (CED). After infusion, distribution volumes were evaluated. The rats with high BP/heart rate displayed a significantly larger distribution of the infused molecules within the injected site and more extensive transport of those molecules to the globus pallidus. This difference was particularly apparent for AAV2, for which a 16.5-fold greater distribution of viral capsids was observed in the rats with high BP/heart rate than in the rats with no heartbeat. Similar results were observed for liposomes, despite their larger diameter. The distribution of all infused molecules in all rats that had low or no blood flow was confined to the space around brain blood vessels. These findings show that fluid circulation within the CNS through the perivascular space is the primary mechanism by which viral particles and other therapeutic agents administered by CED are spread within the brain and that cardiac contractions power this process.

Keywords

perivascular space; AAV2; liposomes; brain; transport; convection-enhanced delivery

INTRODUCTION

Direct delivery of drugs and viral vectors to the central nervous system (CNS) is a promising approach to molecular and genetic therapies for neurological diseases, but optimal distribution requires better definition of the brain's microanatomy and fluid dynamics to clarify the principles governing delivery and flow of macromolecules within the CNS. Among hypotheses

*To whom correspondence and reprint requests should be addressed Fax: +1 415 514 2864. piotr.hadaczek@ucsf.edu.

for the distribution of viral vectors in the brain [1–8], natural anatomical boundaries and possibly degree of tissue myelination are thought to play a role. In highly myelinated areas with compact cellular structure (e.g., cortex), vector is concentrated close to the injection needle. In areas with laminar structure (e.g., hippocampus), transgene expression is more widespread [9,10]. Transgene protein product may also be detected a substantial distance from the injection site—a finding often interpreted to indicate neuronal transport along specific pathways [2,6,11–13].

Simple diffusion within brain parenchyma has been considered the primary mechanism of distribution of therapeutic molecules with agents infused manually [14–17]. Convection-enhanced delivery (CED) has recently proved an efficient, practical technique for targeting brain structures [15,18,19]. Infusion is performed by maintaining a pressure gradient over a much longer time than is possible with manual injection. CED permits an even distribution of solutes while preventing reflux. The use of co-infusates (e.g., heparin [19,20], basic fibroblast growth factor [21], or mannitol [22]) or alternating osmotic pressure within brain parenchyma can enhance distribution.

We found that CED results in widespread distribution of viral agents within rodent and monkey brain tissue [18,20,23]. We attributed the distribution to CED-induced bulk flow of fluid within brain parenchyma and neuronal transport of the agents, but on observing unusual distribution patterns, we examined the distribution more closely. CED of liposomes [24] or AAV2 vector [15] into rodent brain and CED of AAV2-AADC (aromatic L-amino acid decarboxylase) vector into monkey striatum [23] produced a pattern in which the agent was concentrated around blood vessels.

Perivascular spaces are extensions of the subarachnoid spaces associated with vessels that penetrate the brain down to the level of capillaries. The concept of the perivascular space as a conduit for the distribution of molecules within the CNS is not new [25–28]. Rennels *et al.* [27] showed that solutes in cerebrospinal fluid (CSF) have rapid access to the extracellular space throughout the neuraxis by way of fluid pathways paralleling the parenchymal vasculature. This work demonstrated that horseradish peroxidase tracer remains largely in the perivascular space and the network of extracellular channels. Blocking pulsation of the cerebral arteries with aortic occlusion or partial ligation of the brachiocephalic artery prevented the rapid paravascular influx of tracer [27,29]. This apparently convective influx of tracer was thus facilitated by transmission of the pulsation of the cerebral arteries to the microvasculature. While the perivascular spaces are primarily pathways for the drainage of soluble and insoluble material from the brain, those findings and our more recent observations suggested that they may also be important in transporting therapeutics within the CNS.

To test the hypothesis that interstitial infusion of macromolecules into brain parenchyma results in their rapid spread along the perivascular space, propelled by pulsing of the heart as a mechanism of transport within brain tissue, we infused three entities—AAV2, liposomes, and bovine serum albumin—into rat striatum by CED. We compared the pattern and volume of distribution (V_d) of the molecules in anesthetized rats with either high blood pressure (BP) and heart rate (induced by epinephrine) or low BP and heart rate (induced by blood withdrawal) and in rats euthanized just before the infusion (no heart action). As heart action contributed substantially to broad distribution of the molecules, we proposed that the pulse acts as a pump to distribute particles infused into the interstitium of the brain along the conduit of the perivascular space to sites deeper in the parenchyma and remote in the brain. Although differences in distribution among molecules depend on their specific physicochemical properties, our results suggest that the “perivascular pump” can play an important role in the delivery of potentially therapeutic molecules to the CNS.

RESULTS

Distribution Patterns in Rat Brain

We infused three agents into the striatum of the rats by means of CED: AAV2 capsids (25 nm in diameter), small unilamellar liposomes (65 nm), and bovine serum albumin (7.2 nm). We analyzed their distribution patterns and V_d within the brain with a fluorescence technique. For each infused agent, three groups were created: H—high BP/heart rate rats (epinephrine-induced), L—low BP/heart rate rats (induced by blood withdrawal), and N—no heart action rats (euthanized immediately before infusion) (Table 1). After anesthesia or euthanasia, we infused rat brains with one of the three agents; for groups H and L, the infusion started when the mean BP was maintained at more than 110 mm Hg and less than 60 mm Hg, respectively. We analyzed the V_d of fluorescent particles or compounds according to the protocol described under Materials and Methods. We made comparisons among the three groups of rats.

Bovine Serum Albumin

Infusion of fluorescein 5′-isothiocyanate (FITC)-labeled bovine serum albumin into the striatum showed the highest V_d in group H (15.3 ± 1.5 mm^3). The corresponding values were 11.1 ± 0.95 mm^3 for group L and 2.8 ± 0.3 mm^3 for group N. In the globus pallidus (GP), the V_d for H was 5.4 ± 0.5 mm^3, for L was 2.7 ± 0.25 mm^3, and for N was 1.0 ± 0.15 mm^3. In all three groups of rats, V_d in the rats infused with albumin were higher than the corresponding values in the rats infused with AAV2 or liposomes (Fig. 1).

Liposomes

The infusion of neutral liposomes into the brains of group H rats resulted in a robust distribution within both the striatum and the GP. V_d in those rats were similar to those obtained for bovine serum albumin: 14.0 ± 1.0 mm^3 for striatum and 4.8 ± 0.37 mm^3 for GP. As before, the rats with low BP/heart rate and with no heart action showed significantly lower V_d: in group L, 4.6 ± 0.32 mm^3 for striatum and 0.42 ± 0.05 mm^3 for GP, and in group N, 1.8 ± 0.1 mm^3 for striatum and 0.3 ± 0.06 mm^3 for GP (Fig. 1).

AAV2

Immunostained sections from the brains of group H rats infused with AAV2 capsids showed an average V_d of 3.3 ± 0.2 mm^3 in the striatum and 1.9 mm^3 ± 0.2 mm^3 in the GP. In group L rats, the V_d in the striatum was 0.75 ± 0.07 mm^3, whereas we detected no staining in the GP. In group N rats, the striatal V_d was 0.2 ± 0.02 mm^3 and there was no signal in the GP. It appeared that, without adequate blood flow, AAV2 particles were not transported from their injection site in the striatum to the GP. The ratio of the viral V_d in the striatum between groups H and N was 16.5 to 1.0 (Fig. 1).

Statistical Comparison of Groups H, L, and N

In general, the distribution of all three agents tested was enhanced within the brain when a high BP and heart rate were maintained during infusion compared to no heartbeat or when a low BP was sustained. Although we used bovine serum albumin (7.2 nm) as a small, neutral, control molecule, the V_d of the liposomes (65 nm) was almost identical in both groups of rats with a high BP/heart rate (H and L). In the rats with no heart action (N), however, the V_d of liposomes was approximately 1.5 times lower than that of albumin in the striatum (2.8 mm^3 versus 1.8 mm^3) and more than 3 times lower in the GP (1 mm^3 versus 0.3 mm^3). Without the action of the heart, only the pressure from CED infusion pushed the labeled entities through the brain parenchyma. Under such circumstances, large liposomes (65 nm in diameter) spread less widely than did the albumin. Indeed, in group H, the V_d of AAV2 was 4.6 times lower than that of albumin (3.3 mm^3 versus 15.3 mm^3). However, in the rats with no heart action, that

ratio was 14 times greater (0.2 mm^3 versus 2.8 mm^3). Relative comparisons and their statistical significance for the infused substances within each group of rats are shown in Fig. 1.

As for the pattern of distribution, the fluorescent signal obtained from all infused molecules was distinctly different in the brains of the rats that had no heart action (N) and those with low BP/heart rate (L). In both of those groups, the signal was confined to, and was dotted around, the blood vessels in the brain rather than spread evenly (Fig. 2E–2H and Fig. 3E–3H). Such a truncated distribution was evident in the brain sections of all rats in groups L and N, whereas we saw a more global distribution in the sections from group H rats, those with a high BP/heart rate (Fig. 2A–2D and Fig. 3A–3D). That phenomenon was especially pronounced in group N, the rats with no heart action, and to a lesser extent, in group L, the rats with decreased BP/heart rate.

DISCUSSION

Robust and controlled distribution of therapeutic agents within targeted brain regions is a key aspect of any approach to gene or molecular therapy. Different strategies and manipulations have been suggested to enhance and optimize the delivery of drugs into the CNS [15,19–22, 30,31]. CED of viral vectors in gene therapy systems has shown great promise as a delivery strategy. Because CED affords a controlled pressure gradient during infusion, substances of various sizes have all shown V_d as large as several cubic centimeters in the brain tissue of both rats and rhesus monkeys [31]. High drug concentrations can be achieved at specific sites by this method, but to optimize the benefits of CED, its underlying mechanisms must be defined by gaining more detailed knowledge about the anatomical and physiological features of the brain that govern delivery.

The synapse has dominated concepts of neuronal communication and has been a paradigm for understanding patterns of viral spread within the brain. Neuronal transport has long been postulated for viruses and virus-derived vectors used in gene therapy for the CNS. Recognized axonal pathways are believed to be responsible for transporting viral particles like the pseudorabies virus [6,12], herpes simplex virus [11], or AAV [1] from one region of the brain to another. Kaspar *et al.* [2] injected AAV containing the reporter gene green fluorescent protein (GFP) into rat hippocampus and striatum. After 2 weeks, they observed GFP expression in brain regions retrogradely connected to the sites of injection—cortical entorhinal layer II neurons for the hippocampus and substantia nigra for the striatum. They suggested that axonal retrograde transport of viral particles had occurred.

In our experience with viral vector delivery to the CNS, we have often observed that cellular transduction is confined to the space around blood vessels in the brain. This observation raised the possibility that viral particles might be spread within the brain by a simple, non-neuronal pathway within the CNS.

In previous experiments in rats (unpublished data), we injected AAV2 into striatum; rats were euthanized rapidly after injection and the brains processed for immunohistochemical evaluation with anti-AAV2 antibody (A20). We detected viral capsids in the GP immediately after injection. This apparently immediate and distant spread of AAV further suggested the presence of a rapid non-neuronal mechanism of transport within the brain. Observing such a fast time course, we directed our attention to the possibility of a fluid mechanism and to the brain's perivascular spaces.

It is known that CSF extends into the perivascular (Virchow–Robin) spaces. These spaces are an extension of the subarachnoid space that accompanies penetrating arteries into the brain down to the level of capillaries [32]. Within this space, metabolites and small solutes can diffuse quite freely between extracellular fluids and CSF. The concept of a perivascular space system

has been studied in detail, and the existence of a pathway for rapid flow of CSF from the subarachnoid space into the perivascular spaces has been confirmed [25–27]. The movement of fluid is caused by arterial pulsation resulting from normal heart action. We therefore tested the hypothesis that the natural heartbeat could contribute to the distribution and transport of intracranially infused molecules within those spaces.

Our results confirm a rapid spread of molecules that cannot be explained by diffusion as the sole mechanism. Even bovine serum albumin—the smallest substance we used—has a molecular weight of 66 kDa and is too large to diffuse freely in the intracranial environment. In group N rats, with no heartbeat, the V_d of albumin was approximately 5.5 times less in both the striatum and the GP than in group H rats, with a high BP/heart rate. The V_d of liposomes and AAV2 particles was even more dependent on heart action, with V_d in the striatum almost 8 times greater for the liposomes and 16.5 times greater for AAV2 in group H versus group N. In addition, distribution of all three agents in the brain of rats with either no (group N) or slow (group L) heart action showed a much more confined and spotty fluorescent signal, which was found entirely around blood vessels. All of these observations are consistent with the hypothesis that agents are propelled within the perivascular conduit by a pulsatile (peristaltic) mechanism. A normal heartbeat generates a periodic traveling wave of wall deformation in the outer wall of the artery, with its amplitude and velocity contributing to the spread of infusates within the brain tissue. However, the effect should be more pronounced in larger vessels, such as arterioles, and become greatly diminished or absent in very small capillaries.

Comparing differences among the agents used, one phenomenon deserves particular comment. We invariably observed the largest V_d with bovine serum albumin, which seems logical because it is a natural and pH-neutral composite of circulating serum that has no charge and is much smaller than the other two agents used. Comparing control albumin with AAV2, in group H, with high blood flow, we noticed much poorer spread of viral capsids within both the striatum (4.6 times less; 15.3 mm^3 versus 3.3 mm^3) and the GP (approximately 2.8 times less; 5.4 mm^3 versus 1.9 mm^3). Yet the greatest discrepancies were detected when we analyzed the striatal distributions of AAV2 in group N, with no heart action, or group L, with low blood flow, and compared them with those in group H infused with control albumin. The relative fold differences in V_d were 76.5 (0.2 mm^3 versus 15.3 mm^3) and 20.4 (0.2 mm^3 versus 0.75 mm^3), respectively. When we made similar comparisons only within the albumin-infused animals, those differences were strikingly smaller—only 5.5-fold less V_d for group N and 1.4-fold less for group L. It is tempting to speculate that this finding was a result of the large difference in size between the albumin molecule (7.2 nm) and the AAV2 particle (25 nm), as larger molecules distribute less widely than smaller ones. However, when liposomes—which are even larger than AAV2 particles—were infused the V_d was comparable to that of albumin. The liposomes, despite their relatively larger size (65 nm), distributed far better than the smaller viral particles. We must seek factors other than size to explain these differences in distribution. Affinity for the surrounding cellular membranes is one possibility. AAV2 has an extremely high affinity for its cellular receptor heparan sulfate proteoglycan, which is found on all neurons. It seems reasonable to assume that migration of AAV2 particles is retarded by these tissue receptors during infusion. Immobilized on the neuronal membrane, they cannot travel as easily as can neutral liposomes or albumin molecules. This conclusion is consistent with the observation that co-infusion of heparin with AAV2 greatly improves distribution [20]. This is another example of the efficiency of liposomes for delivery of therapeutic agents within the CNS.

We also evaluated transport patterns from the site of infusion to other parts of the brain. Spread outside the striatum was seen only in the GP, located caudal to the striatum. Other investigators have also described this phenomenon [1,33,34], although most evaluated transgene expression

immunohistochemically, which leaves uncertain what was actually transported—the protein product of the transgene, the viral genetic material, or intact viral particles.

We detected the transport of viral capsids immediately after infusion. Within 30 min, AAV2 was transported to the GP. The pallidal capsid distribution was limited and confined by the anatomic boundaries of that structure. The GP in rat forms a physically encapsulated brain region and the fluorescent signal was restricted precisely to that oval territory. There is a strict and specific connection of a brain microvasculature between striatum and GP, so—aside from the natural anatomical brain organization—the vascular system connecting those two structures must also be taken into consideration. It was interesting to find that the spread and transport of all molecules studied were detected only in the GP and not in any frontal parts of the brain. This finding reflects the direction of blood flow in the basal ganglia circuit, in which the movements caused by arterial pulsation are directed caudally. In determining how much agent entered the striatum compared with the GP, the V_d ratio was almost 2:1 (1.7-fold difference) in group H (3.3 mm^3 versus 1.9 mm^3), whereas we could not detect any signal at all in the GP of the rats in groups L (low BP/heart rate) or N (no heart action). This finding further supports our concept of a “perivascular pump” distributing and transporting viral particles within the CNS. When that pump was “switched off,” all capsids were trapped by cellular receptors at the site of infusion, from which even the pressure from CED could not propel them to the neighboring GP. In contrast, albumin and liposome signals did appear in the GP, even in the rats with no heart action—probably because these are neutral molecules with no natural receptors that might entrap them. The CED pressure gradient was enough to push them, at least to some extent, through the perivascular space to the adjacent brain structure.

The mechanism responsible for propulsion by perivascular pump is not well understood. We speculate that, with each pulse, the artery wall expands and that this arterial expansion moves downstream in the direction of the systolic blood pressure wave, thereby moving perivascular fluid downstream. Arterial “undulation” depends on the expansion and contraction of the arterial wall with each pulse, which depends not only on how much the heart contracts, but also on the resistance of the circuit defined by diameter and elasticity of the blood vessel. Most likely, resistance is highest distally (at the level of arterioles and capillaries—the most arborized portions of the vascular tree), whereas elasticity is highest more proximally. Perivascular pumping appears to depend on the expansion of the arterial wall, which is closely related to pulse pressure (PP), defined as the difference between systolic and diastolic pressure. In group H, PP was 77 (150 – 73), and in group L, only 25 (72 – 47). In fact, PP may be considered the most informative for perivascular pump performance. The lower the PP, the weaker the effectiveness of the perivascular pump. It is noteworthy that, with the onset of arteriosclerosis, the artery walls become more rigid, the amplitude of pulsations is reduced, and the passage of fluid along the vessel walls is impaired. Thus, regardless of the arterial pressure, there might, under some circumstances, be no fluid flow outside the blood vessel. That, in fact, is the key foundation of capillary and arterial cerebral amyloid angiopathy in Alzheimer disease (AD). Overproduction of amyloid β (Aβ), entrapment of Aβ in drainage pathways, and poor drainage of Aβ from the aging brain appear to play a major role in the pathogenesis of AD. Functional changes in the aging cerebral vasculature might be involved in the accumulation of amyloid peptides in brain parenchyma and in vessel walls. Disturbance of blood vessel tone and pulsations could be a factor in the deposition of Aβ in artery walls. Loss of elasticity in aging cerebral arteries with progressive arteriosclerosis, or cessation of pulsations, might play a role in impeding the drainage of Aβ and pathogenesis of cerebral amyloid angiopathy. This possibility has been studied broadly by Weller *et al.* [35–37]. It seems that a mechanism similar to that responsible for drainage of Aβ from the brain may also be responsible for spreading viral vectors and other therapeutic molecules after local brain delivery, as demonstrated in this study.

GENERAL CONCLUSIONS

Our observations in rats with no heart action are fully consistent with the mechanism first suggested by the work of Rennels *et al.* [27] and Stoodley *et al.* [29]. We postulate that fluid circulation through the CNS occurring via the perivascular space is the primary mechanism by which viral particles and other therapeutic agents administered by CED are spread within the brain. Cardiac contractions are necessary to power this process. The first computational *in vitro* model of the perivascular space system has already been proposed [38]. A detailed understanding of all the conditions influencing perivascular fluid flow is of great importance in predicting the time, direction, and, eventually, the efficiency of therapeutic molecule transport. It is conceivable that manipulation with drugs and substances with cerebral vasomotor properties may offer another option for optimizing the delivery and distribution of therapeutic molecules within the CNS. It is not clear which aspect of blood flow is more critical for powering the perivascular pump—heart rate or blood pressure. Choosing more specific drugs to manipulate those functions independently could further elucidate the mechanism and importance of the brain fluid circulation to the transport of viral vectors and other molecules within the brain.

MATERIALS AND METHODS

Experiments were performed with 27 male Sprague–Dawley rats (Charles River Laboratories, Wilmington, MA, USA) weighing 250–300 g. All procedures were approved by and in accordance with the regulations of the Institutional Animal Care and Use Committee of the University of California at San Francisco.

Study design

To examine the distribution of AAV2 particles, liposomes, and bovine serum albumin within the rat striatum and GP under the study conditions, we assigned the rats to nine study groups (Table 1).

AAV2

Recombinant AAV2 virions harboring humanized GFP (hGFP) under the control of a hybrid promoter consisting of the cytomegalovirus enhancer fused to the chicken β-actin promoter (CBA) were packaged in the helper-virus-free system using the pDG plasmid (generously provided by Juergen Kleinschmidt, University of Heidelberg) and 293 cells as described previously, with minor modifications [39–41]. Fast performance liquid chromatography was used to purify the virus on a POROS-PI ion-exchange column (Waters, Milford, MA, USA) followed by a HiTrap heparin column (Amersham Biosciences, Piscataway, NJ, USA) as described previously [41,42]. The titer of rAAV-CBA-hGFP was 4.5×10^{13} vg/ml as determined by real-time polymerase chain reaction, and the percentage of packaged particles was ~80% as determined by electron microscopy by previously published methods [43,44]. The concentration of AAV2 capsids used for striatal infusion was 5.6×10^{13} capsids/ml.

Liposomes

Liposomes were prepared by lipid-film hydration using Hepes-buffered saline (pH 6.5) as the hydration buffer. The sample was hydrated in six successive cycles of freezing (−80°C) and thawing (60°C). Unilamellar liposomes were formed by extrusion using a 10-ml-capacity thermostatically controlled extruder (Northern Lipids, Vancouver, BC, Canada). Extrusion was performed through polycarbonate membranes of an appropriate pore size, and the number of extrusions required to reach the desired liposome size (approximately 65 nm) was determined by light scattering (Beckman Coulter, Fullerton, CA, USA). Cholesterol was obtained from Calbiochem (San Diego, CA, USA). 1,2-Dioleoyl-*sn*-glycero-3-phosphocholine (DOPC) and

1,2-distearoyl-*sn*-glycero-3-phos-phoethanolamine-*N*-[methoxy(polyethylene glycol)-2000] (PEG-DSPE) were purchased from Avanti Polar Lipids (Alabaster, AL, USA). Liposomes were composed of a 3/2 (mol/mol) phospholipid/cholesterol mixture. DOPC was used as the phospholipid component and the PEG-DSPE quantity was 10% (mol/mol) of the total phospholipid in this study. $DiIC_{18}$-liposomes were labeled with membrane-bound $DiIC_{18}$ fluorescence—1,1′-dioctadecyl-3,3,3′3′-tetramethylindocarbocyanine perchlorate (Sigma, St. Louis, MO, USA) having two C_{18} chains. The $DiIC_{18}$ content was 1% (mol/mol) of total phospholipids. For the infusion study, liposome concentrations were 2 μM phospholipid.

Surgery

The rats were anesthetized with isoflurane (Baxter, Deerfield, IL, USA) (3 L mixed with oxygen) and were placed in a small-animal stereotactic frame (David Kopf Instruments, Tujunga, CA, USA). A sagittal skin incision was made, and burr holes were made in the skull by twist drill, 0.5 mm anterior to the bregma and 3 mm to the right and left of the midline. All infusions were performed by CED. AAV2 particles, liposomes, or albumin in a 5-μl solution was infused into each hemisphere (Table 1). To minimize trauma and reflux, customized needle cannulae were created by inserting silica capillary tubing (100 μm in diameter; Polymicro Technologies, Phoenix, AZ, USA) into a 24-gauge needle fused with a Teflon tube (0.02 in.) and connected to a programmable microinfusion pump (Bioanalytical Systems, West Lafayette, IN, USA). The loading chamber (Teflon tubing, 1/16 in. o.d. × 0.03 in. i.d.) and attached infusion chamber (1/16 in. o.d. × 0.02 in. i.d.) were filled with 60 μl of each mixture per loading line. Two cannulae (one per hemisphere) were placed in the rat striatum, 5 mm below the dura. The infusion rate was 0.2 μl/min for 10 min and 0.5 μl/min for 6 min. The infusions in rats with no heart action (N) were initiated when no heartbeat was detected with a stethoscope placed below the rat torso after a lethal injection of sodium pentobarbital (50 mg/kg). The two other groups of rats were closely monitored during surgery to maintain either high BP (H) or low BP (L). We used the CyQ BMP02 system (CyberSense, Inc., Nicholasville, KY, USA), which was designed to monitor invasively systolic, diastolic, pulse pressure, and mean arterial BP. This system includes a Deltran BP transducer that can precisely measure arterial vasomotor parameters. BP measurements were made by placing an intravenous catheter (24 gauge × 3/4 in.; 0.67 (0.47 i.d.) (Terumo Medical Corp.) in the femoral artery (standard protocol at http://www.cyq.com/htdocs/femoral_artery_catheter.html). Plastic tubing attached to a three-way stopcock was used and connected with two 3-ml syringes. One was filled with phosphate-buffered saline (PBS) and heparin (100 U/ml) to rinse the tubing to avoid blood coagulation; the other contained epinephrine solution (as bitartrate) 1:50,000 (Abbott Laboratories, North Chicago, IL, USA). For the high-BP group, the epinephrine solution was slowly injected. When mean BP exceeded 110 mm Hg, vector infusion was started. Further injections of epinephrine were made whenever the mean BP dropped below 110 mm Hg. For the low BP group, about 1.5 ml of blood was withdrawn into the syringe, and when the mean BP dropped below 60 mm Hg, vector infusion was initiated. The measurements were recorded every 30 s for all four values (systolic, diastolic, mean BP, heart rate/min). Table 2 shows the average readings from cardiovascular measurements of those two groups of animals. They were euthanized immediately after infusion.

AAV2 group

Rats in this group were transcardially perfused with sterile 0.01 M phosphate buffered saline (PBS). The brains were rapidly removed. Left hemispheres of rats in groups H and L were separated from the right hemispheres (infused with liposomes) and postfixed overnight in 4% paraformaldehyde solution (for group N, the whole brain was postfixed without separating hemispheres because AAV2 was infused in both striata). The left hemispheres (groups H and L), and whole brains from group N, were then washed and transferred to a series of 10, 20, and 30% sucrose solutions in 0.01 M PBS for cryopreservation. They were cut into 40-μm serial

coronal sections on a cryostat. Frozen sections were collected in a series in antifreeze solutions and stored at −70°C Every fifth section from the AAV2 groups was stained for immunohistochemical evaluation. After a wash in PBS, the sections were incubated in blocking solution (1% normal goat serum and 0.01% Triton X-100 in PBS) for 30 min, followed by incubation in primary antibody solution (mouse monoclonal anti-AAV antibody A20—1:40; American Research Products, Inc., Belmont, MA, USA) overnight at room temperature. After being washed three times in PBS, sections were reacted for 1 h with goat FITC-conjugated anti-mouse immunoglobulin G secondary antibody (concentration 1:100; Jackson ImmunoResearch, West Grove, PA, USA). After being washed three times in PBS, sections were mounted onto slides, covered with antifading agent, and then covered with glass coverslips. Prepared tissues were analyzed with fluorescence microscopy.

Liposome and albumin groups

As both the bovine serum albumin and the liposomes infused into the rat hemispheres were labeled with fluorescent dyes (FITC-conjugated albumin and 1,1′-dioctadecyl-3,3,3′,3-tetramethylindocarbocyanine-5,5′-disulfonic acid incorporated in DOPC-based 65-nm liposomes), the sections did not require any additional staining. Freshly removed brains (for liposomes, the right hemispheres of groups H and L and whole brains from group N; for albumin, the whole brains of groups H, L, and N) were immediately frozen in isopentane in dry ice. Subsequently, brains were cut into 25-μm serial, coronal sections on a cryostat and were mounted directly on positively charged slides. Every eighth section was analyzed with fluorescence microscopy (Axioskop, Zeiss, Germany) with an FITC filter for the albumin and a TRITC filter for the liposomes. The distance between analyzed sections was 200 μm.

Image analysis

The V_d of AAV2 capsids, liposomes, and FITC-labeled albumin were analyzed with a Macintosh-based image analysis system (NIH ImageJ 1.34s; Bethesda, MD, USA). Images of fluorescence in brain slices were captured by a CCD camera and Adobe PhotoShop software (Adobe Systems, Inc., San Jose, CA, USA). With the NIH Image analysis software, the area of distribution of infused particles or compounds in each tissue section was determined automatically at a 50% threshold of the maximum stained optical density. The sum of the areas of infusion was used to determine the V_d in each striatum and GP. Quantification was performed on every fifth serial section for the AAV2 group and on every eighth section for the albumin and liposome groups (a distance of 200 μm between analyzed sections) by the Cavalieri method [45] under ×2.5 magnification.

Statistical analysis

To compare distributions, sections were aligned independently according to the injection site for each side. After V_d was calculated for each group studied, results were expressed as mean volumes with the corresponding standard deviation. Student's t test was used to determine statistical significance. Differences were considered statistically significant at the level of $P \leq 0.05$.

ACKNOWLEDGMENTS

This work was supported by National Institutes of Health Award U54NS045309. Special thanks to Lisa Tesch (Northwestern University, Chicago, IL, USA) for preparing the AAV vector and Susan Eastwood ELS(D) (University of California at San Francisco ret.), who edited the manuscript. We are also grateful to John Forsayeth (University of California at San Francisco) for helpful discussions concerning preparation and organization of the manuscript.

REFERENCES

1. Chamberlin NL, Du B, de Lacalle S, Saper CB. Recombinant adeno-associated virus vector: use for transgene expression and anterograde tract tracing in the CNS. Brain Res 1998;793:169–175. [PubMed: 9630611]
2. Kaspar BK, et al. Targeted retrograde gene delivery for neuronal protection. Mol. Ther 2002;5:50–56. [PubMed: 11786045]
3. Tsiang H. Evidence for an intraaxonal transport of fixed and street rabies virus. J. Neuropathol. Exp. Neurol 1979;38:286–299. [PubMed: 86604]
4. Lascano EF, Berria MI. Histological study of the progression of herpes simplex virus in mice. Arch. Virol 1980;64:67–79. [PubMed: 6246857]
5. Kristensson K, Nennesmo L, Persson L, Lycke E. Neuron to neuron transmission of herpes simplex virus: transport of virus from skin to brainstem nuclei. J. Neurol. Sci 1982;54:149–156. [PubMed: 6281393]
6. Yang M, Card JP, Tirabassi RS, Miselis RR, Enquist LW. Retrograde, transneuronal spread of pseudorabies virus in defined neuronal circuitry of the rat brain is facilitated by gE mutations that reduce virulence. J. Virol 1999;73:4350–4359. [PubMed: 10196333]
7. Gerendai I, Toth IE, Boldogkoi Z, Medveczky I, Halasz B. Central nervous system structures labelled from the testis using the transsynaptic viral tracing technique. J. Neuroendocrinol 2000;12:1087–1095. [PubMed: 11069124]
8. Enquist LW, Card JP. Recent advances in the use of neurotropic viruses for circuit analysis. Curr. Opin. Neurobiol 2003;13:603–606. [PubMed: 14630225]
9. McCown TJ, Xiao X, Li J, Breese GR, Samulski RJ. Differential and persistent expression patterns of CNS gene transfer by an adeno-associated virus (AAV) vector. Brain Res 1996;713:99–107. [PubMed: 8724980]
10. Chen H, McCarty DM, Bruce AT, Suzuki K. Oligodendrocyte-specific gene expression in mouse brain: use of a myelin-forming cell type-specific promoter in an adeno-associated virus. J. Neurosci. Res 1999;55:504–513. [PubMed: 10723060]
11. Sun N, Cassell MD, Perlman S. Anterograde, transneuronal transport of herpes simplex virus type 1 strain H129 in the murine visual system. J. Virol 1996;70:5405–5413. [PubMed: 8764051]
12. Husak PJ, Kuo T, Enquist LW. Pseudorabies virus membrane proteins gI and gE facilitate anterograde spread of infection in projection-specific neurons in the rat. J. Virol 2000;74:10975–10983. [PubMed: 11069992]
13. Bohn MC, et al. Adenovirus-mediated transgene expression in nonhuman primate brain. Hum. Gene Ther 1999;10:1175–1184. [PubMed: 10340549]
14. Galvin KA, Oorschot DE. Continuous low-dose treatment with brain-derived neurotrophic factor or neurotrophin-3 protects striatal medium spiny neurons from mild neonatal hypoxia/ischemia: a stereological study. Neuroscience 2003;118:1023–1032. [PubMed: 12732247]
15. Cunningham J, et al. Distribution of AAV-TK following intracranial convection-enhanced delivery into rats. Cell Transplant 2000;9:585–594. [PubMed: 11144956]
16. Blaha GR, Raghupathi R, Saatman KE, McIntosh TK. Brain-derived neurotrophic factor administration after traumatic brain injury in the rat does not protect against behavioral or histological deficits. Neuroscience 2000;99:483–493. [PubMed: 11029540]
17. Proescholdt MA, et al. Vascular endothelial growth factor (VEGF) modulates vascular permeability and inflammation in rat brain. J. Neuropathol. Exp. Neurol 1999;58:613–627. [PubMed: 10374752]
18. Bankiewicz KS, et al. Convection-enhanced delivery of AAV vector in parkinsonian monkeys: in vivo detection of gene expression and restoration of dopaminergic function using pro-drug approach. Exp. Neurol 2000;164:2–14. [PubMed: 10877910]
19. Hamilton JF, et al. Heparin coinfusion during convection-enhanced delivery (CED) increases the distribution of the glial-derived neurotrophic factor (GDNF) ligand family in rat striatum and enhances the pharmacological activity of neurturin. Exp. Neurol 2001;168:155–161. [PubMed: 11170730]

20. Nguyen JB, Sanchez-Pernaute R, Cunningham J, Bankiewicz KS. Convection-enhanced delivery of AAV-2 combined with heparin increases TK gene transfer in the rat brain. Neuroreport 2001;12:1961–1964. [PubMed: 11435930]
21. Hadaczek P, Mirek H, Bringas J, Cunningham J, Bankiewicz K. Basic fibroblast growth factor enhances transduction, distribution, and axonal transport of adeno-associated virus type 2 vector in rat brain. Hum. Gene Ther 2004;15:469–479. [PubMed: 15144577]
22. Mastakov MY, Baer K, Xu R, Fitzsimons H, During MJ. Combined injection of rAAV with mannitol enhances gene expression in the rat brain. Mol. Ther 2001;3:225–232. [PubMed: 11237679]
23. Eberling JL, et al. In vivo PET imaging of gene expression in parkinsonian monkeys. Mol. Ther 2003;8:873–875. [PubMed: 14664788]
24. Mamot C, et al. Extensive distribution of liposomes in rodent brains and brain tumors following convection-enhanced delivery. J. Neurooncol 2004;68:1–9. [PubMed: 15174514]
25. Gregory TF, Rennels ML, Blaumanis OR, Fujimoto K. A method for microscopic studies of cerebral angioarchitecture and vascular-parenchymal relationships, based on the demonstration of ‘paravascular’ fluid pathways in the mammalian central nervous system. J. Neurosci. Methods 1985;14:5–14. [PubMed: 4033188]
26. Rennels ML, Blaumanis OR, Grady PA. Rapid solute transport throughout the brain via paravascular fluid pathways. Adv. Neurol 1990;52:431–439. [PubMed: 2396537]
27. Rennels ML, Gregory TF, Blaumanis OR, Fujimoto K, Grady PA. Evidence for a ‘paravascular’ fluid circulation in the mammalian central nervous system, provided by the rapid distribution of tracer protein throughout the brain from the subarachnoid space. Brain Res 1985;326:47–63. [PubMed: 3971148]
28. Cserr HF, Ostrach LH. Bulk flow of interstitial fluid after intracranial injection of blue dextran 2000. Exp. Neurol 1974;45:50–60. [PubMed: 4137563]
29. Stoodley MA, Brown SA, Brown CJ, Jones NR. Arterial pulsation-dependent perivascular cerebrospinal fluid flow into the central canal in the sheep spinal cord. J. Neurosurg 1997;86:686–693. [PubMed: 9120633]
30. Mastakov MY, Baer K, Kotin RM, During MJ. Recombinant adeno-associated virus serotypes 2- and 5-mediated gene transfer in the mammalian brain: quantitative analysis of heparin co-infusion. Mol. Ther 2002;5:371–380. [PubMed: 11945063]
31. Lieberman DM, Laske DW, Morrison PF, Bankiewicz KS, Oldfield EH. Convection-enhanced distribution of large molecules in gray matter during interstitial drug infusion. Neurosurg 1995;82:1021–1029.
32. Lennart, H. The Human Brain and Spinal Cord: Functional Neuroanatomy and Dissection Guide. Vol. 2nd ed.. New York: Springer-Verlag; 1995. p. 506
33. Kordower JH, et al. Neurodegeneration prevented by lentiviral vector delivery of GDNF in primate models of Parkinson’s disease. Science 2000;290:767–773. [PubMed: 11052933]
34. Tenenbaum L, et al. Tropism of AAV-2 vectors for neurons of the globus pallidus. Neuroreport 2000;11:2277–2783. [PubMed: 10923685]
35. Nicoll JA, Yamada M, Frackowiak J, Mazur-Kolecka B, Weller RO. Cerebral amyloid angiopathy plays a direct role in the pathogenesis of Alzheimer’s disease. Pro-CAA position statement. Neurobiol. Aging 2004;25:589–597. [PubMed: 15172734]
36. Preston SD, Steart PV, Wilkinson A, Nicoll JA, Weller RO. Capillary and arterial cerebral amyloid angiopathy in Alzheimer’s disease: defining the perivascular route for the elimination of amyloid beta from the human brain. Neuropathol. Appl. Neurobiol 2003;29:106–117. [PubMed: 12662319]
37. Weller RO, et al. Cerebral amyloid angiopathy: amyloid beta accumulates in putative interstitial fluid drainage pathways in Alzheimer’s disease. Am. J. Pathol 1998;153:725–733. [PubMed: 9736023]
38. Bilston LE, Fletcher DF, Brodbelt AR, Stoodley MA. Arterial pulsation-driven cerebrospinal fluid flow in the perivascular space: a computational model. Comput. Methods Biomech. Biomed. Eng 2003;6:235–241.
39. Grimm D, Kern A, Rittner K, Kleinschmidt JA. Novel tools for production and purification of recombinant adenoassociated virus vectors. Hum. Gene Ther 1998;9:2745–2760. [PubMed: 9874273]

40. Zolotukhin S, et al. Production and purification of serotype 1, 2, and 5 recombinant adeno-associated viral vectors. Methods 2002;28:158–167. [PubMed: 12413414]

41. Jiang L, et al. Tight regulation from a single tet-off rAAV vector as demonstrated by flow cytometry and quantitative, real-time PCR. Gene Ther 2004;11:1057–1067. [PubMed: 15152187]

42. Kaludov N, Handelman B, Chiorini JA. Scalable purification of adeno-associated virus type 2, 4, or 5 using ion-exchange chromatography. Hum. Gene Ther 2002;13:1235–1243. [PubMed: 12133276]

43. Veldwijk MR, et al. Development and optimization of a real-time quantitative PCR-based method for the titration of AAV-2 vector stocks. Mol. Ther 2002;6:272–278. [PubMed: 12349826]

44. Gao G, et al. Purification of recombinant adeno-associated virus vectors by column chromatography and its performance in vivo. Hum. Gene Ther 2000;11:2079–2091. [PubMed: 11044910]

45. Cavalieri, B. Geometria Degli Indivisible. Turin: Unione Tipografica Editrice; 1996.

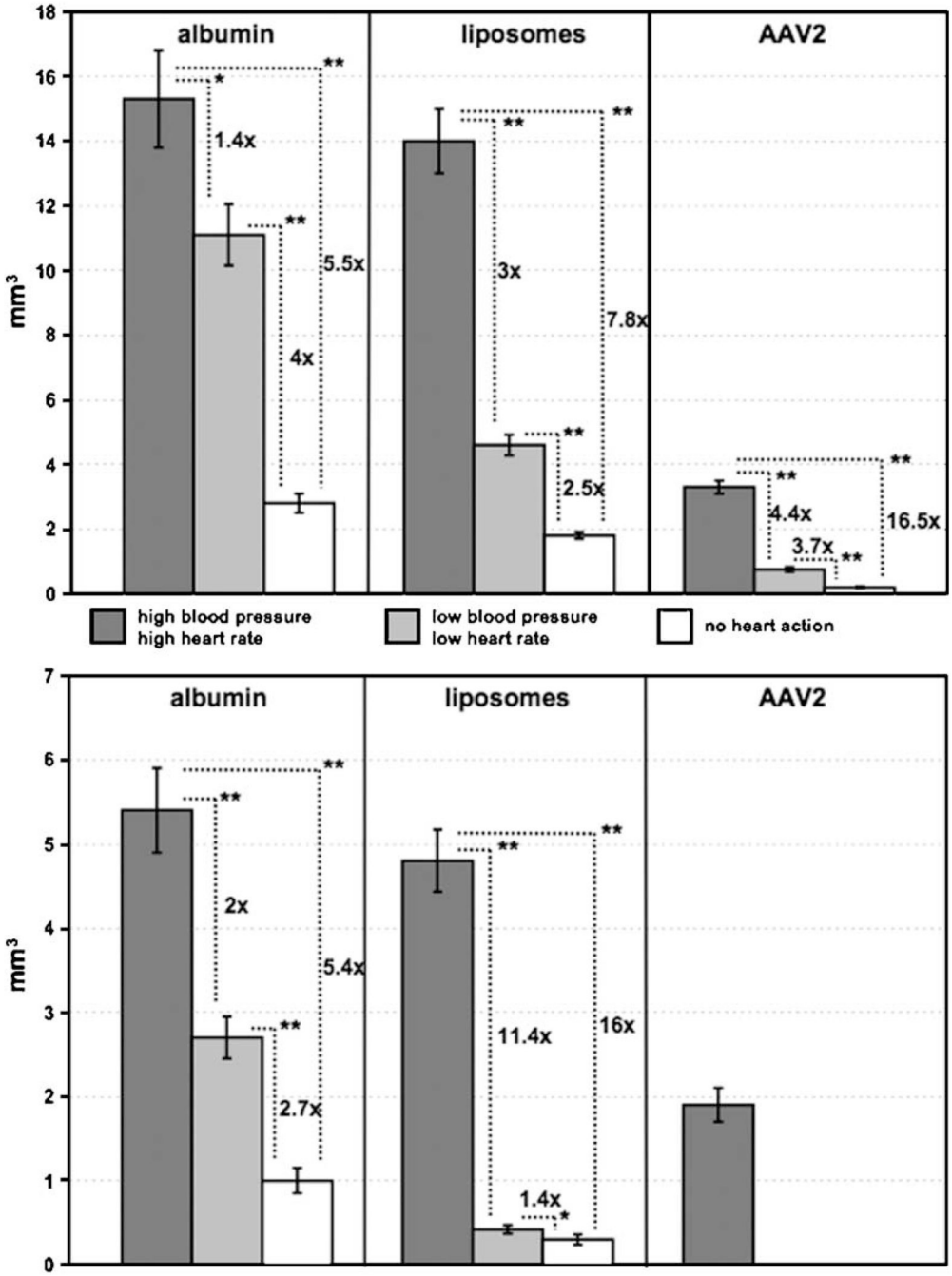

FIG. 1.

Volumes of distribution (V_d) of three substances infused into rat striatum (top) and distributed from there into the globus pallidus (bottom). Dark-shaded columns represent values for group H (high blood pressure/heart rate). Light-shaded columns represent values from group L (low blood pressure/heart rate). White columns represent values for group N (rats with no heart action). Standard deviation bars are shown on each column. Statistically significant differences in both the striatum and the globus pallidus among rats infused with the different molecules are shown as relative differences with $*P < 0.009$ and $**P < 0.00005$. Of interest is that the striatal V_d of liposomes in group H was almost identical to that of bovine serum albumin. AAV2

distribution was significantly less due to entrapment of viral capsids by heparan sulfate proteoglycan receptors widely present on neurons [20].

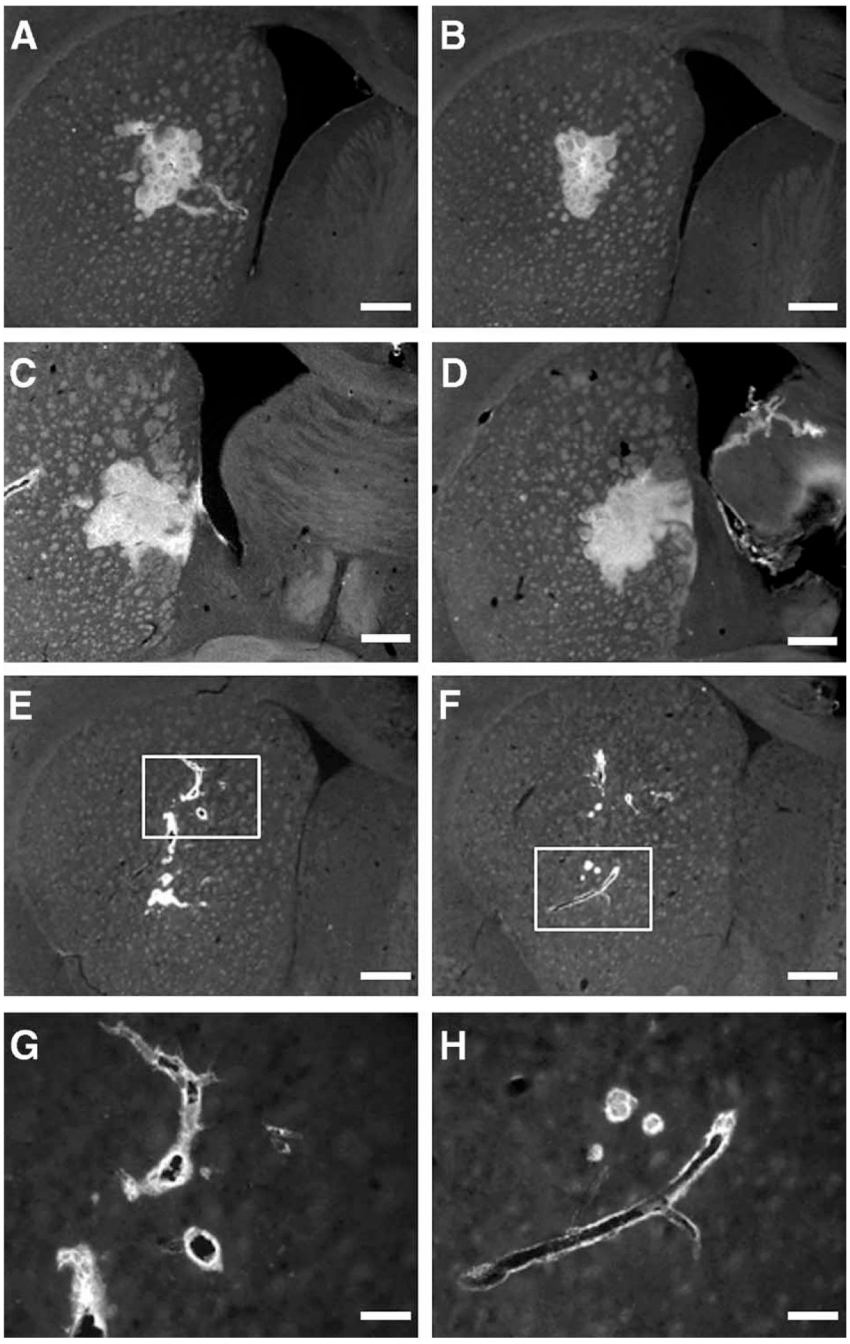

FIG. 2.

Photographs of brain sections stained for AAV2 capsids (antibody A20) in rats after intrastriatal infusion of AAV2 by convection-enhanced delivery. (A and B) Striatal sections from two different rats from group H (high blood pressure/heart rate); (C and D) brain sections from a more caudal part of the same brains showing positive signal in globus pallidus. For all rats from group H, the fluorescent signal was spread evenly within the hemisphere, forming a mostly uninterrupted distribution. (E and F) Brain sections from two rats with low blood pressure/heart rate when AAV2 was infused. The signal is restricted to the vicinity of infusion and the perivascular area surrounding nearby blood vessels. (G and H) Higher magnification

views of E and F (original magnification ×20). Size bars: 500 (A through F) and 125 μm (G and H).

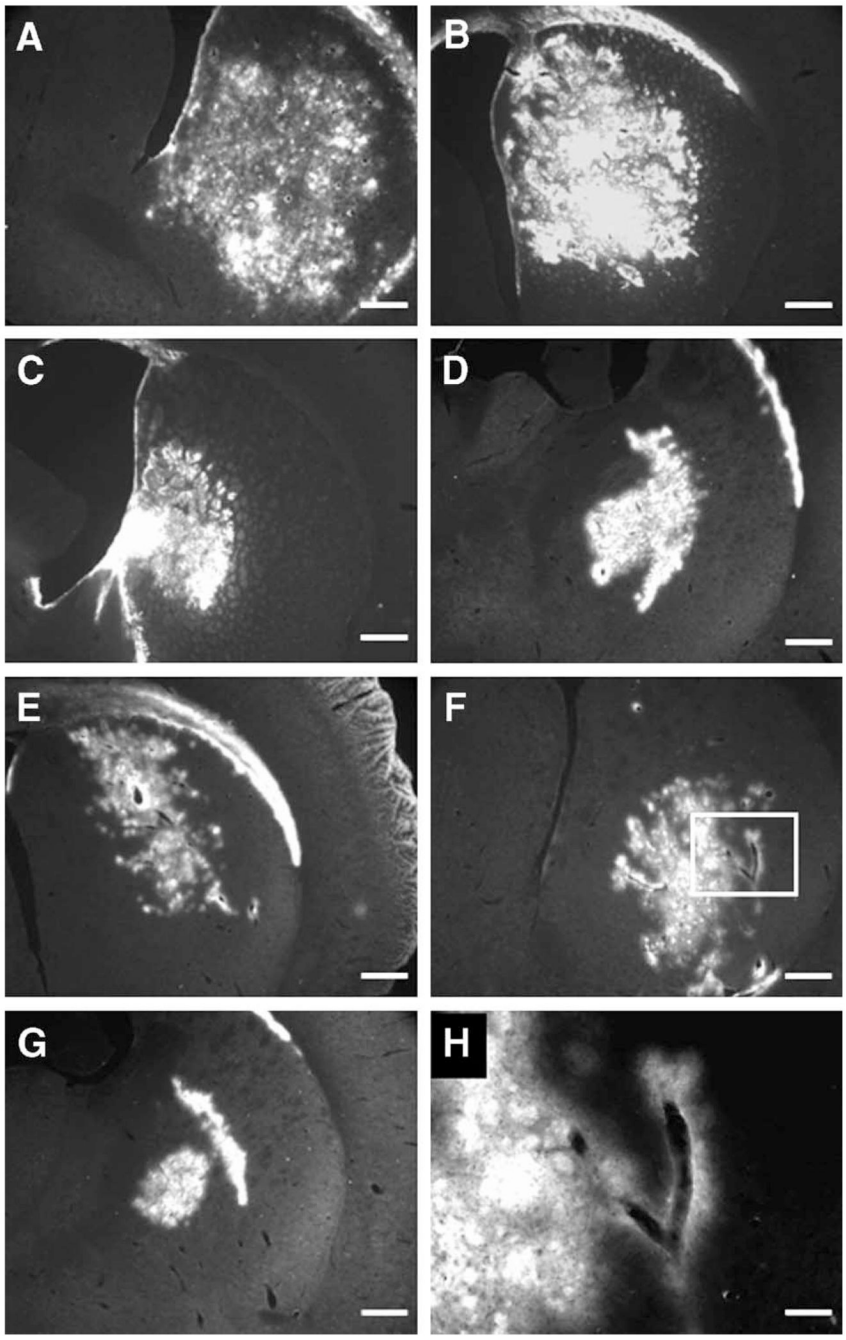

FIG. 3.

Sections from rat brains infused with fluorescent liposomes. (A through D) Note the robust and widespread liposomal distribution within the striatum (A and B) and globus pallidus (C and D) of rats from group H (high blood pressure/heart rate). This signal pattern forms a fairly continuous area of fluorescence. (E and F) Striatal sections from rats from group L (low blood pressure/heart rate). Note the arborized pattern of spread suggesting perivascular pathways. (G) Brain section from a more caudal part of the brain from a rat from group L showing signal confined in the globus pallidus. (H) Higher magnification view of F (original magnification ×20). Size bars: 500 (A–G) and 125 μm (H).

TABLE 1

Study groups and conditions for intrastriatal infusions in rats by CED

Study groups and conditions	BSA	Liposomes	AAV2
Group H, high blood pressure/ heart rate	3 rats (both hemispheres)	6 rats (right hemisphere)	6 rats (left hemisphere)
Group L, low blood pressure/ heart rate	3 rats (both hemispheres)	6 rats (right hemisphere)	6 rats (left hemisphere)
Group N, no heart action	3 rats (both hemispheres)	3 rats (both hemispheres)	3 rats (both hemispheres)
CED infusate	BSA-FITC conjugate (0.5 ng)	Dil-DS 65-nm liposomes (200 nM)	AAV2-hGFP (5.6×10^{13}capsids/ml)

All rats received 5-μl infusions per hemisphere at the following rates: 0.2 μl/min for 10 min and 0.5 μl/min for 6 min. CED, convection-enhanced delivery; BSA, bovine serum albumin; FITC, fluorescein 5'-isothiocyanate; Dil-DS, 1,1′-dioctadecyl-3,3,3′,3′-tetramethylindocarbocyanine-5,5′-disulfonic acid; AAV2, adeno-associated virus 2; hGFP, humanized green fluorescent protein.

TABLE 2

Measurements of arterial blood pressure (BP) and heart rate in rats with high blood pressure (group H) and rats with low blood pressure (group L)

Group H			Group L		
Systolic : diastolic	Mean BP	Heart rate/min	Systolic : diastolic	Mean BP	Heart rate/min
150 ± 10 : 73 ± 10	111.5	341 ± 22	72 ± 4 : 47 ± 4	59.5	255 ± 12